DIGITAL COMPUTATION OF THE FRACTIONAL MELLIN TRANSFORM

Edip Biner and Olcay Akay

Dokuz Eylül University, Department of Electrical and Electronics Engineering
Kaynaklar Campus, 35160 Buca / IZMIR TURKEY
E-mail: edip.biner@eee.deu.edu.tr , olcay.akay@eee.deu.edu.tr

ABSTRACT

In this paper, we develop an algorithm to compute the fractional Mellin transform (FrMT). The connection between the FrMT and the fractional Fourier transform (FrFT) is formed by the logarithmic warping operator $\mathbf{U}_{\log}$. Following this connection, we first develop an algorithm to perform the logarithmic warping operation which is combined together with a discrete FrFT algorithm to compute the FrMT. Performance of the developed algorithm is demonstrated through simulations.

1. INTRODUCTION

The fractional Mellin transform (FrMT) is a generalization of the scale covariant transform [1] and the Mellin transform on the scale-warped time-frequency plane [2]. The definition of the FrMT was inspired by the previously defined fractional Fourier transform (FrFT), which is a generalization of the identity and the classical Fourier transforms on the time-frequency plane [3]. Using the unitary equivalence concept of Baraniuk and Jones [4], a theoretical definition of the FrMT was given in [2]. A similar definition appeared in [5].

In this work, we develop a discrete-time algorithm of the FrMT proposed in [2]. The FrMT of a time domain signal s(t) is derived [2] as in (1) at the bottom of the page. In (1), $\mathbb{M}$ denotes the FrMT operator and the symbol is an angle parameter. The FrMT is well suited to analyze signals whose frequency varies hyperbolically with time. Examining the kernel of the transformation in (1), the instantaneous frequency of these signals can be expressed as

$$f_i(t) = \frac{\ln t}{t}\cot + \frac{1}{t}\frac{\hat{m}}{\sin} \qquad (2)$$

In (2), $\hat{m}$ and are the fractional scale and angle parameters, respectively, that determine the shape of the instantaneous frequency curves of the signal. The localization of these signals in the time-frequency plane are illustrated in Fig. 1. In Fig 1(a), $\hat{m}$ takes on the values $\hat{m}_7 < \hat{m}_6 < \hat{m}_5 < \hat{m}_4 = 0 < \ldots < \hat{m}_1$ while is fixed as /2. In Fig 1(b), assumes the values $_7 < _6 < _5 < 0 < _4 < _3 < _2 < _1 = /2$ as $\hat{m}$ is kept constant at 0.

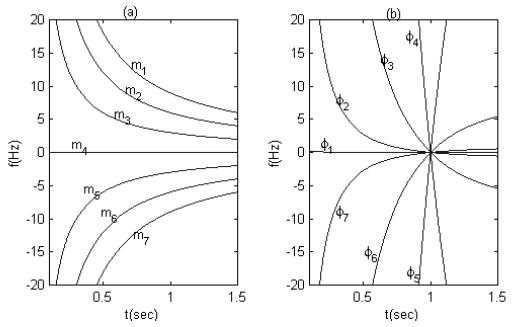

Fig. 1 Instantaneous frequency curves of the signals suited to analysis with the FrMT. In (a) $\hat{m}$ is varied while is kept constant whereas in (b) is varied while $\hat{m}$ is fixed.

The hyperbolic nature of the instantaneous frequency given in (2) suggests the possibility of using the FrMT in the analysis of mammalian echolocation signals and the hyperbolic frequency modulations propagating through a dispersive underwater channel.

When $=0$, the FrMT reduces to the scale covariant transform in [1]. Similarly, for $= /2$, the FrMT simplifies to the classical Mellin transform. Although the FrMT formulation in (1) appears complicated at first glance, it has been shown in [2] that this formulation can alternatively be expressed as

$$(\mathbb{M}\, s)(m) = \begin{cases} \sqrt{1 \quad j\cot}\, e^{j\ m^2\cot} \quad _0 s(t) e^{j\ (\ln t)^2\cot \quad j2\ (\ln t) m\csc} \dfrac{dt}{\sqrt{t}}, & n \\ e^{\frac{m}{2}} s(e^m), & = (2n) \\ e^{\frac{m}{2}} s(e^{\ m}), & = (2n+1) \end{cases} \qquad (1)$$

$$(\mathbb{M}\ s)(m) = (\mathbb{F}\ \mathbf{U}_{\log} s)(m). \qquad (3)$$

In (3), $\mathbb{F}$ denotes the FrFT operator [3] defined at the angle parameter . $\mathbf{U}_{\log}$ is called the logarithmic warping operator and is defined [4] as

$$(\mathbf{U}_{\log} s)(t) = e^{t/2} s(e^t). \qquad (4)$$

This operator takes signals with support regions in the positive time axis and stretches their support region onto the whole real time axis. Note that the logarithmic warping operator changes not only the argument but also the amplitude of the signal in a time dependent manner.

According to (3), computing the FrMT of a continuous time signal s(t) is equivalent to first applying the logarithmic warping $\mathbf{U}_{\log}$ and then computing the FrFT of the logarithmically warped signal. Our discrete FrMT algorithm is based on the equivalence relation in (3). Since there already exists algorithms to implement the FrFT [6] - [8], development of a logarithmic warping algorithm to implement $\mathbf{U}_{\log}$ is sufficient to calculate the FrMT.

The concept of scale and scale related transforms have previously been addressed in several papers in the literature. A discrete version of the classical Mellin transform was developed by Bertrand et. al. [9]. Cohen defined and established the scale transform that can be considered a special case of the classical Mellin transform [10]. Later, Zalubas and Williams proposed [11] a discrete implementation of Cohen's scale transform. However, to our knowledge, an algorithm for the digital computation of the *fractional* Mellin transform (FrMT) has not been proposed.

2. DEVELOPMENT OF THE FrMT ALGORITHM

2.1 Logarithmic Warping Algorithm

In this section we discuss the algorithmic implementation of the logarithmic warping operator, $\mathbf{U}_{\log}$, given in (4). Note that $\mathbf{U}_{\log}$ has a time dependent formula. Hence, to be able to calculate the logarithmically warped version of a signal s(t) one needs complete knowledge of the time support of s(t). It is assumed that the signal is sampled at a rate of $f_s = \sqrt{2N}$ where N is the number of samples in the analyzed signal. This is dictated by the constraints of the particular FrFT algorithm [6] that we employ in our FrMT algorithm. We first construct the vector of sampling instances t[n] of the sampled analyzed signal s[n]. For each instance t[i] in t[n], the warped value $s[e^{t[i]}]$ is calculated by interpolation. The warping operation for each sample is completed by a final multiplication of $s[e^{t[i]}]$ by $e^{t[i]/2}$ as indicated in (4).

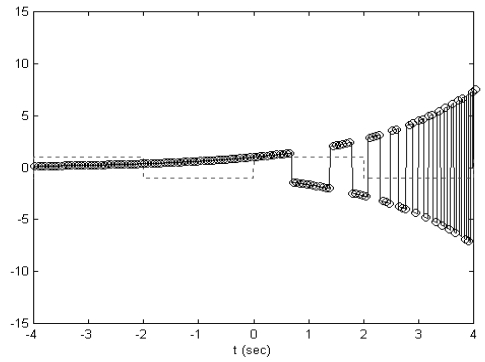

Fig. 2 Logarithmic warping of a square wave.

Performance of the warping algorithm is demonstrated in Fig. 2 where the solid line represents the theoretical logarithmic warping of the square wave represented by the dashed line. The data points shown by the circles are the sample values obtained by our logarithmic warping algorithm described above. For this particular example, we employed linear interpolation; however, depending on the type of the signal to be warped different interpolation schemes such as cubic spline can be utilized. In the simulations that follow, we employed cubic spline interpolation.

One unavoidable shortcoming of the proposed logarithmic warping algorithm is that it requires a large number of samples of the original analyzed signal to produce a warped signal with reasonable number of samples. For an unwarped signal of N samples the algorithm can only produce $2\ln^2(\frac{N}{8})$ samples of the warped signal. This is because of the exponential function that forms the argument of the warped signal in (4). In Fig. 2, we used an original signal with 32768 samples to produce a warped signal of length 138.

2.2 Implementation of the FrMT Algorithm

Combining the logarithmic warping algorithm with the discrete-time FrFT algorithm in [6] as in (3) provides a practical way to compute the FrMT of time domain signals. Using the inverse logarithmic warping operator, $\mathbf{U}_{\log}^{-1}$, together with (3), we can write

$$(\mathbb{M}\ \mathbf{U}_{\log}^{-1} s)(m) = (\mathbb{F}\ \mathbf{U}_{\log}\mathbf{U}_{\log}^{-1} s)(m) = (\mathbb{F}\ s)(m). \qquad (5)$$

In (5), $\mathbf{U}_{\log}^{-1}$ is given as

$$(\mathbf{U}_{\log}^{-1} s)(t) \quad \tfrac{1}{\sqrt{t}} s(\ln t). \qquad (6)$$

We use the equality in (5) to test the validity of our FrMT algorithm. As an example, we use an inverse logarithmically warped complex exponential signal,

$$(\mathbf{U}_{\log}^{-1} s)(t) = [\mathbf{U}_{\log}^{-1}\{e^{j2\ f_0 t}\}](t) = \tfrac{1}{\sqrt{t}} e^{j2\ f_0 \ln t}. \qquad (7)$$

We can easily write the theoretical FrMT of the inverse logarithmically warped complex exponential in (7) using the relationship in (5) along with FrFT tables [3]

$$[\mathbb{M}\ \mathbf{U}_{\log}^{-1}s](m) = (\mathbb{F}\ s)(m) = \sqrt{1+j\tan\ }\ e^{\ j\ (m^2+f_0^2)\tan\ +j2\ mf_0\sec} \tag{8}$$

which is plotted in Fig. 3 using solid line. We used f_0=1 and = /12 radians. We also computed the FrMT of (7) by first applying the logarithmic warping algorithm described in Section 2.1 followed by the discrete-time FrFT algorithm [6] as indicated in the middle part of (5). The data points shown by circles in Fig. 3 are the result of our discrete FrMT algorithm. Theoretical and algorithmic results match to a great degree. Small deviations near the end points could be attributed to the approximate nature of the FrFT algorithm [6].

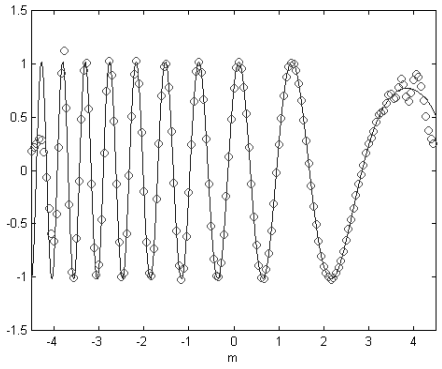

Fig. 3 Comparison of the theoretical FrMT of (7) (solid) with the discrete FrMT using our algorithm (circles).

2.3 A Signal Separation Application Using the FrMT

To demonstrate the utility of our algorithm, we include a signal separation application involving the FrMT. Consider the signal

$$s(t) = \frac{1}{\sqrt{t}}(5e^{\ (\ln(t))^2} + e^{j[\ \ (\ln(t))^2+2\ \ f_0\ln(t)]}) \tag{9}$$

which is formed by adding inverse logarithmically warped Gaussian and chirp signals. The two warped signals are superimposed in such a way that an easy separation of them in time domain is not feasible.

Using our discrete FrMT algorithm we calculated the FrMT of the signal in (9) assigning parameter values of = 1 and $f_0 = 6$. The angle value of the FrMT is taken as =atan( )+ /2. Notice that the angle parameter is matched with the sweep rate parameter, , of the warped chirp signal. The magnitude of the FrMT signal is plotted in Fig. 4. It can be observed that the inverse logarithmically warped chirp signal is localized as an impulse, thanks to the transform angle matching the sweep rate of the chirp signal. The Gaussian signal can easily be separated by applying a simple multiplicative mask of width 2 centered around the origin of the fractional scale domain. This masking operation effectively zeroes out the impulse due to the warped chirp signal that we want to separate from the warped Gaussian. To go back to time domain, the inverse FrMT of the masked Gaussian signal is computed using the relationship

$$(\mathbb{M}\ )^{-1} = (\mathbb{F}\ \mathbf{U}_{\log})^{-1} = \mathbf{U}_{\log}^{-1}\mathbb{F} \tag{10}$$

where we used the inverse property of the FrFT given as [3]

$$(\mathbb{F}\ )^{-1} = \mathbb{F}\ . \tag{11}$$

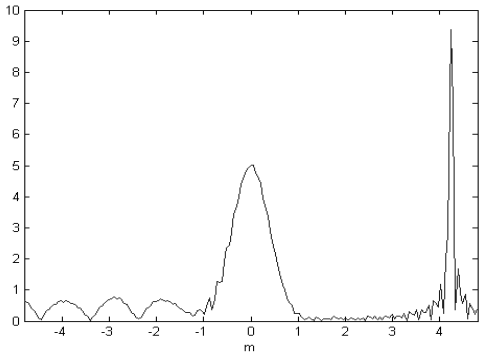

Fig. 4 FrMT of s(t) in (9) computed at the matching angle value =atan( )+ /2.

According to (10), the inverse FrMT corresponds to first computing the FrFT at angle – and then applying the inverse logarithmic warping operator $\mathbf{U}_{\log}^{-1}$. The inverse logarithmic warping algorithm is implemented using interpolation analogously to its forward version. The recovered time domain signal after computing the inverse FrMT is plotted using solid line in Fig. 5. The dashed line shows the original warped Gaussian signal in (9).

It can be seen that the original and recovered signals agree to a great degree. This signal separation experiment can also be performed in a noisy environment successfully.

2.4 An Example of FrMT versus FrFT

As a last demonstration, we compute and compare the FrMT and FrFT of a rectangular pulse signal as shown in Fig. 6. In Fig. 6(a) through Fig. 6(d), the FrFT of the rectangular pulse is illustrated on the top subplot while the FrMT is illustrated on the bottom. Fig. 6(a) through Fig. 6(d) depict the magnitude parts of both transforms computed at =0, /6, /3, and /2 radians, respectively.

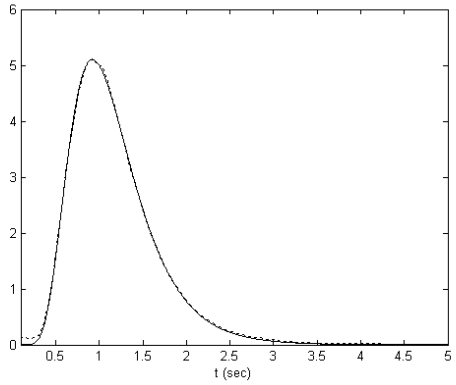

Fig. 5 Comparison of the recovered warped Gaussian (solid) with the original warped Gaussian (dashed).

Notice that the bottom subplot of Fig. 6(a) corresponds to the logarithmically warped rectangular pulse. As the transform angle increases towards /2, both transforms move towards the origin while the transform magnitudes continuously evolve into sinc functions. We would like to stress that the subplots in Fig. 6(d) correspond to the classical Fourier transforms (= /2) of the signals in the respective subplots of Fig. 6(a). Due to the symmetry property of the Fourier transform, both transforms in Fig. 6(d) are centered at the origin.

MATLAB scripts of all the simulations can be obtained from http://www.eee.deu.edu.tr/~biner/frmt/frmt.zip.

3. CONCLUSION

We proposed a discrete implementation of the FrMT based on (3). For that purpose, we first developed a logarithmic warping algorithm employing interpolation. The FrMT algorithm was realized by first applying the logarithmic warping on the analyzed signal and then computing the FrFT of the warped signal using the discrete FrFT in [6]. The performance of the algorithm was demonstrated through simulations. Our FrMT algorithm works quite well, as indicated in the examples. However, it requires a large number of samples of the analyzed signal, as dictated by the restrictions of the digital FrFT algorithm, to produce a reasonable number of samples of the FrMT.

4. REFERENCES

[1] R. G. Baraniuk, "A signal transform covariant to scale changes", *IEE Electr. Lett.*, vol. 29, pp. 1675-1676, Sept. 1993.

[2] O. Akay and G. F. Boudreaux-Bartels, "Fractional Mellin transform: An extension of fractional frequency concept for scale", *8th DSP Workshop,* (in CD-ROM), 1998.

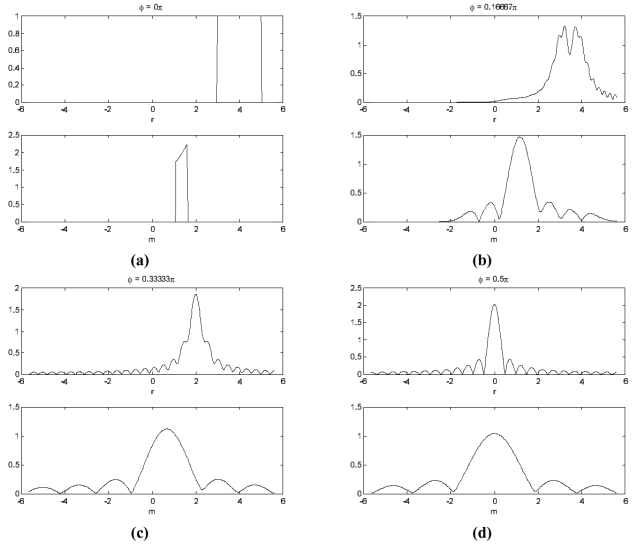

Fig. 6 The FrFT (top) and the FrMT (bottom) of a rectangular pulse at different angles between 0 to /2.

[3] L. B. Almeida, "The fractional Fourier transform and time-frequency representations", *IEEE Trans. on Sig. Proc.,* vol. 42, no. 11, pp. 3084-3091, Nov. 1994.

[4] R. Baraniuk and D. Jones, "Unitary equivalence: A new twist in signal processing", *IEEE Trans. on Sig. Proc.*, vol. 43, no. 10, pp. 2269-2282, Oct. 1995.

[5] A. I. Zayed, "A class of fractional integral transforms: A generalization of the fractional Fourier transform", *IEEE Trans. on Sig. Proc.*, vol. 50, no. 3, pp. 619-627, March 2002.

[6] H. M. Ozaktas, O. Arikan, M. A. Kutay and G. Bozdagi, "Digital computation of the fractional Fourier transform", *IEEE Trans. on Sig. Proc.,* vol. 44, no. 9, pp. 2141-2150, Sept. 1996.

[7] C. Candan, M.A. Kutay, and H.M. Ozaktas, "The discrete fractional Fourier transform", *IEEE Trans. on Sig. Proc.*, vol. 48, no. 5, pp. 1329-1337, May 2000.

[8] S. Pei, M. Yeh and C. Tseng, "Discrete fractional Fourier transform based on orthogonal projections", *IEEE Trans. on Sig. Proc.*, vol. 47, no. 5, pp. 1335-1348, May 1999.

[9] J. Bertrand, P. Bertrand and J. P. Ovarlez, "Discrete Mellin transform for signal analysis", in *Proc. IEEE Int. Conf. Acoust., Speech and Sig. Process. (ICASSP'90)*, pp. 1603-1606, 1990.

[10] L. Cohen, "The scale representation", *IEEE Trans. on Sig. Proc."*, vol. 41, no. 12, pp. 3275-3292, Dec. 1993.

[11] E. J. Zalubas and W. J. Williams, "Discrete scale transform for signal analysis", in *Proc. IEEE Int. Conf. on Acoust., Speech and Sig. Process. (ICASSP'95),* pp. 1557-1560, 1995.